Eur J Appl Physiol (2001) 85: 214–225
DOI 10.1007/s004210100476

ORIGINAL ARTICLE

Masato Takanokura · Kazuyoshi Sakamoto

Physiological tremor of the upper limb segments

Accepted: 27 April 2001 / Published online: 7 July 2001

Abstract The acceleration signal produced by physiological tremor from four different upper limb segments (the finger, hand, forearm and upper limb) was measured by an acceleration sensor during holding posture and was analyzed by power spectrum analysis. Two prominent peaks appeared in the power spectrum, suggesting that the tremor in the four different limb segments was composed of two frequency components. The frequency of one peak at 8–12 Hz did not change between the different limb segments, while the frequency of the other peak decreased with the increase in the mass of the limb segment. A model with two reflex pathways was developed for the tremor in the four limb segments. The model includes two reflex pathways, a spinal pathway and a supraspinal pathway. The theoretical values of the frequency and the amplitude of the tremor predicted by the model were in good agreement with the experimental results. Analysis of the model revealed that one of the two frequency components of the tremor was of spinal origin and was dependent upon the mass of the limb segment, and the second was of supraspinal origin, corresponding to the frequency at 8–12 Hz. In the normal subject, it is possible that the tremor could be used to evaluate the change in neuromuscular function produced by prolonged work involving just part of a limb segments (e.g., typing). It may also be used to evaluate the neuromuscular function of patients suffering from neurological diseases such as muscular dystrophy and Parkinson's disease.

Keywords Physiological tremor · Upper limb segments · Power spectrum · Model with two reflex pathways

M. Takanokura · K. Sakamoto (✉)
Department of Systems Engineering,
The University of Electro-Communications,
1-5-1 Chofugaoka, Chofu-shi, Tokyo 182-8585, Japan
E-mail: sakamoto@se.uec.ac.jp
Tel.: +81-424-435239
Fax: +81-424-980541

Introduction

An involuntary and continuous oscillation is produced in every part of the human body. In healthy humans, this oscillation is known as physiological tremor (hereafter referred to as tremor). This tremor has been measured in the finger (Halliday and Redfearn 1956; Sakamoto et al. 1992), the hand (Stiles 1976; Hömberg et al. 1987) and the forearm (Matthews and Muir 1980). Although it has been confirmed that the tremor is a periodic oscillation, the frequency of the tremor appears to be dependent upon the limb segment studied. There are two frequency components in the acceleration signal of the finger tremor, as measured by an acceleration sensor (Stiles and Randall 1967; Sakamoto et al. 1992). It has been hypothesized that the two frequency components of the finger tremor originate from the stretch reflex system (via the spinal cord) and the supraspinal system (Lippold 1970; Elble and Randall 1978; Elble and Koller 1990; Sakamoto et al. 1993; Findley and Koller 1995). The supraspinal system includes centers such as the cerebral cortex and the thalamus. The features of the tremor (i.e., the amplitude and the frequency) depend upon the neuromuscular systems involved, including the stretch reflex system and the mechanical system of the limb segment (Elble and Koller 1990; Findley and Koller 1995). It has not yet been investigated how the two frequency components of the tremor differ between upper limb segments. The elucidation of the characteristics of the two frequency components of the tremor for the different limb segments and of the mechanism of the tremor, in terms of the model proposed herein, could be used in the evaluation of the involuntary oscillation observed in other body segments like the lower limb segments and the trunk. In addition, the proposed model for the tremor could contribute to the understanding of the mechanism of the neuromuscular systems under various conditions (e.g., muscular load, fatigue and disease).

In order to investigate the involvement of the different parts of the nervous system and the mechanical system associated with a particular limb segment on the tremor, theoretical considerations have been introduced by using mathematical models. A model for the tremor was first proposed by Stein and Oðuztöreli (1976). They developed a model based on the hypothesis that the tremor was caused by a sensory feedback system and involved the mechanical system of the limb segment. On the basis of their model, another model was proposed by Watanabe and Saito (1984) and Miao and Sakamoto (1995b). These authors postulated that the nervous system consisted of two reflex pathways, the spinal pathway and the supraspinal pathway, and thus included two reflex pathways for the tremor in their model. A model with two reflex pathways was also applied to the tremor; this involved a contribution from the nervous system (Sakamoto et al. 1998) and the addition of a weight load and fatigue (Arihara and Sakamoto 1999b). The theoretical values for the finger tremor predicted by the model were in agreement with the experimental results, but the model for the other limb segments has not yet been studied.

In our previous papers in which we analyzed the finger tremor (Sakamoto et al. 1993; Arihara and Sakamoto 1999a), the origin of the two frequency components of the tremor was investigated by immersion of a finger into water and by changing the weight load on the finger. The 10-Hz frequency component originates chiefly from the supraspinal system, while the other, 20-Hz frequency component is produced by the spinal system. The aim of the present study was to investigate the two frequency components of the tremor in the upper limb segments (i.e., finger, hand, forearm, and upper limb) and to evaluate the two frequency components obtained experimentally with those obtained using a theoretical model with two reflex pathways (hereafter referred to as the tremor model). We also investigated the accuracy of our proposed model.

Experimental study of tremor of various upper limb segments

Methods

Subjects

Ten male students (age range 22–29 years, mean 25.3 years) took part in the experiment. All of the subjects were right-handed and had no neuromuscular system disease.

Experimental procedure

The tremor was measured in four different upper limb segments, the finger, hand, forearm, and upper limb. Figure 1 demonstrates how the tremor was measured in these four limb segments. During all measurements, the subject sat on a chair without a backrest. For the measurement of the finger tremor (Fig. 1a), the subject placed his right hand and forearm on a flat board. The index finger was maintained in a stretched position against gravity. The other fingers remained flat on the board. A marker was put in front of the finger to aid the maintenance of the index finger in a stretched position. For the hand tremor (Fig. 1b), the subject put his right forearm on the board. The hand was maintained in a stretched position against gravity. A marker was put in front of the hand to help the subject to maintain its position. For the forearm tremor (Fig. 1c), the subject put his right elbow on the board. The forearm was placed in a pronated position and maintained in a stretched position against gravity. A marker was also put in front of the forearm to allow the subjects to maintain the position of the arm. During the measurement of the upper limb tremor (Fig. 1d), the right upper limb, which was in a pronated position, was maintained in a stretched position against gravity. The movement of the trunk was eliminated by fixation of the trunk to the wall, and a marker was also placed in front of the upper limb. During measurement, the subject was instructed to maintain the posture described and to gaze at a marker that had been placed at the pointed end of the respective limb segments (Fig. 1). The subject was not provided with any other instruction. The respective limb segments require the use of a different number of joints and agonist muscles, but they were all maintained in the different position (e.g. pronation position). During tremor measurement, therefore, the position of the mechanical ground (i.e., the board and the wall) was different for each of the limb segments, as shown in Fig. 1a–d. The portions of the limb segments from which the tremor was not being measured were kept on the board or the wall. An acceleration sensor was placed in either a distal or proximal position (i.e., not central) on each of the limb segments during tremor measurement (see Fig. 1a–d). The frequency of the tremor for each limb segment was unaffected by the position of the sensor, but the amplitude of the tremor was affected by its position.

Measurement of tremor

The tremor was measured by an acceleration sensor (MT-3 T, Nihon Kohden) for which 170 mV was equal to an acceleration of 1g. That is, the acceleration component of the tremor was evaluated as the tremor. The actual acceleration obtained was in the order of $10^{-2}g$, equivalent to a very small electrical potential (i.e., in the order of a few mV). The measurement period of 60 s was adopted because much longer measurement periods produce an unstable wave for the heavier limb segments. The ratio of the acceleration signal on a limb segment to the signal on the board (i.e., the signal:noise ratio) was found to be 20:1. The sensor was placed on the skin between the distal interphalangeal joint and the distal end of the nail of the index finger for the measurement of the finger tremor (Fig. 1a). For the hand tremor, the sensor was placed on the skin of the dorsal side of the hand, 4 cm from the proximal side measured from the metacarpophalangeal joint of the middle finger (Fig. 1b). For the forearm tremor, the sensor was placed on the skin of the dorsal side of the forearm, 13 cm from the proximal side measured from the wrist joint (Fig. 1c). For the upper limb tremor, the sensor was placed on the skin of the lateral side of the upper limb, 13 cm from the proximal side measured from the elbow joint (Fig. 1d). The placement of the sensor was achieved by using double-faced adhesive tape. The acceleration sensor signal was fed into a bio-amplifier (4214, NEC Sanei) and was recorded on a data recorder (PC-108 M, Sony). During amplification, the acceleration sensor signal was filtered by a band-pass filter with a range of 0.5–1 kHz. The acceleration sensor signal was digitized at a sampling rate of 100 Hz. The digitized data were entered into a personal computer for data analysis.

Data analysis

Power spectrum analysis was performed on the acceleration sensor signal by means of two different methods. First, the power spectrum was estimated by using the fast Fourier transform algorithm (FFT). The total power of the spectrum (i.e., the summation of the

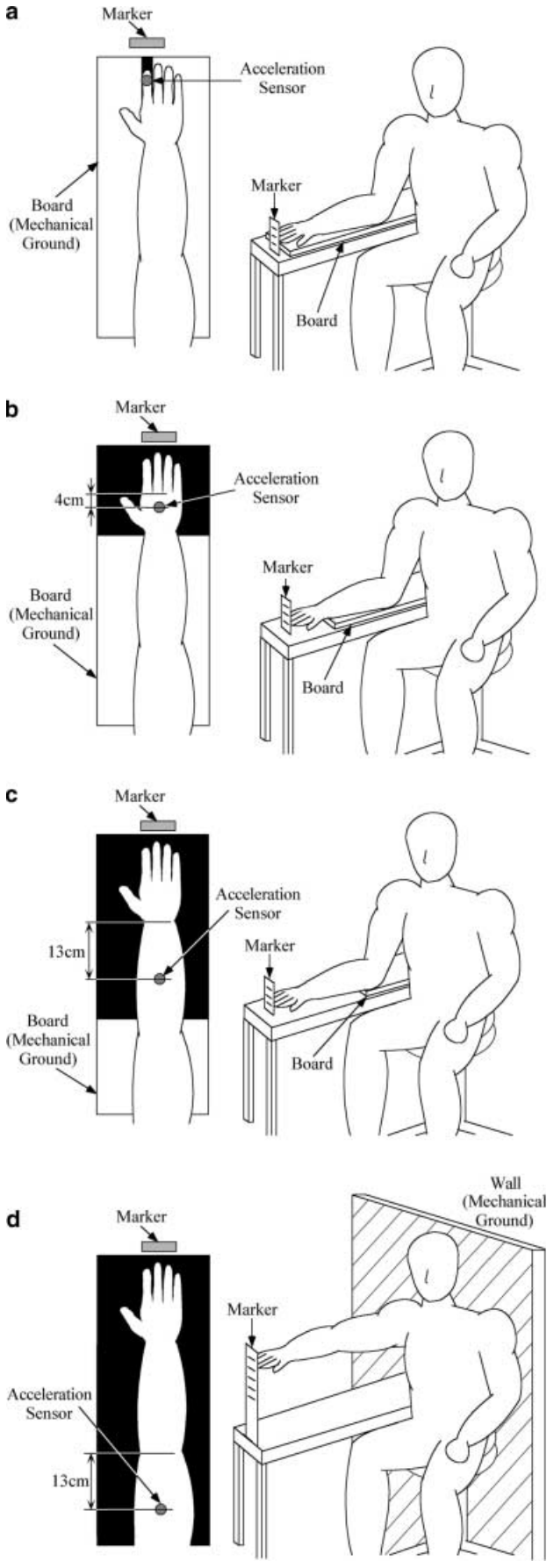

Fig. 1a–d Measurement of tremor in four different limb segments. The right side of each figure illustrates posture of the subject during measurement. A marker was placed in front of each limb segment to allow the subject to maintain its position during measurement of the tremor. The left side shows the limb segment and placement of the acceleration sensor. The *black area* indicates a hole. **a** Finger tremor: the index finger was maintained in a stretched position. **b** Hand tremor: the hand was maintained in a stretched position. **c** Forearm tremor: the forearm was maintained in a stretched pronated position. **d** Upper limb tremor: the upper limb was maintained in a stretched pronated position. The trunk of the subject was fixed to the wall to eliminate movement of the trunk during measurement

power spectrum in the frequency range 0.5–50 Hz) was evaluated. One block of the data used to evaluate one power spectrum consisted of 400 data points (i.e., the data period was 4 s and the sampling time was 10 ms). To guarantee power spectrum statistical reliability, ten blocks of power spectra were averaged. The measured data period was 60 s. In the analysis, the data for the first 20 s were removed because for some of the subjects the data were not stable in that period. The data from 20–60 s were thus used to evaluate the power spectrum. Second, the power spectrum was calculated by using the autoregressive (AR) model (Kay and Marple 1981; Miao and Sakamoto 1995a). Since the acceleration signal of the tremor consisted of the two frequency components, two prominent peaks appeared in the tremor spectrum. The frequencies at the two prominent peaks (i.e., the peak frequencies) were estimated from the tremor spectrum obtained by the AR model.

In the calculation of the AR model, the following procedure was carried out. It was necessary to determine the order of the AR model for the estimation of the power spectrum. In this study, the criterion of Akaike's final prediction error (FPE) was used to determine the order of the AR model (Akaike 1970). Akaike reported that the optimum order for the AR model was chosen as the order at the minimum value of the FPE. Although the optimum order estimated for the FPE was in the range 8–20 for the data obtained in this study, the optimum order depended upon the subject and the limb segment studied. Therefore, the optimum order for the AR model was not taken uniformly, but was determined individually for each of the data sets.

Results

Figure 2a illustrates typical examples of the acceleration sensor signals measured from the four different limb segments studied. Figure 2b shows typical examples of the tremor spectra estimated by FFT. Two prominent peaks appeared in the tremor spectra obtained from all four different limb segments. The frequencies of those peaks were dependent upon the limb segment under investigation. The AR model power spectrum analysis was carried out since clear peaks were observed in the tremor spectra. From the tremor spectrum estimated by the AR model for the experimental data of each subject, the peak frequencies of the two peaks for each subject were first obtained, and then the mean value and the standard deviation (SD) of the peak frequencies for of all the subjects were estimated. The statistical results are displayed in Fig. 3. The two prominent peaks of the tremor spectrum were grouped into two frequency regions. The peak frequency at 8–12 Hz did not change regardless of the limb segment. The other frequency

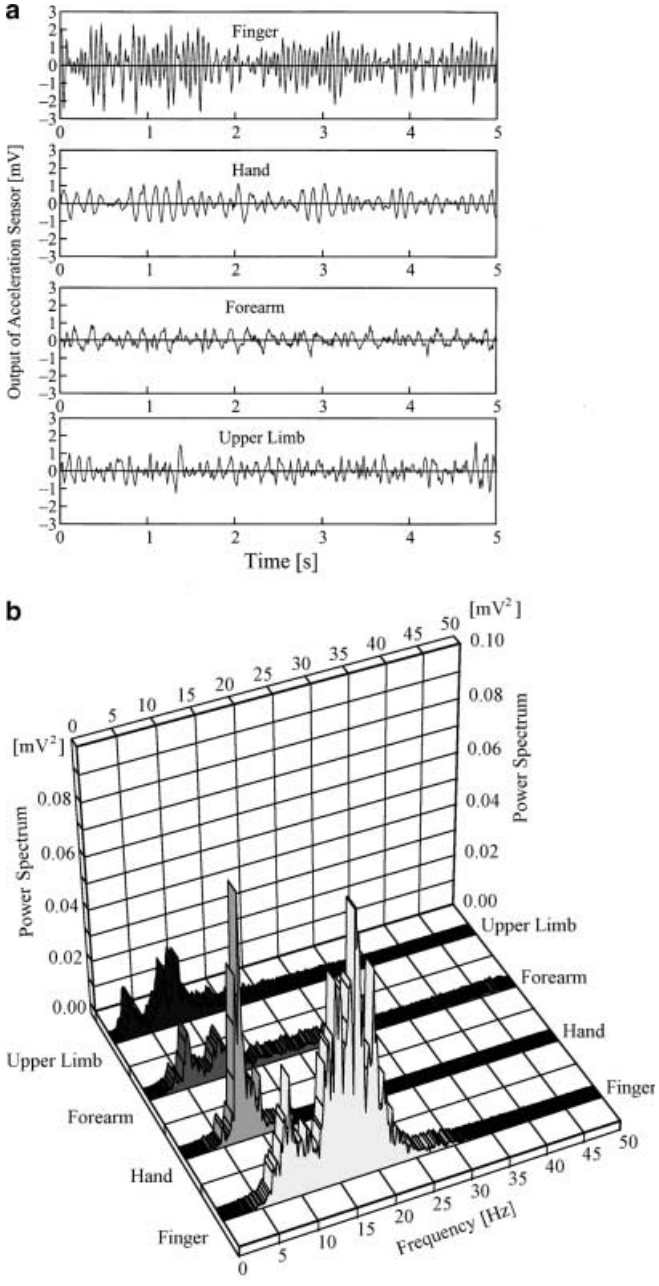

Fig. 2 **a** Examples of acceleration sensor signals measured from the four different limb segments studied. **b** Examples of power spectra of tremor for the four limb segments. Two prominent peaks may be seen in the respective spectra

region had a peak frequency that did depend upon the limb segment.

The amplitude of the tremor for the four different limb segments was evaluated experimentally by the total power of the tremor spectrum in the frequency range 0.5–50 Hz, estimated by FFT. Figure 4 shows the experimental values obtained for the relative total power of the tremor spectrum (crosses) together with the theoretical value predicted by the tremor model described hereafter (closed circles). The total power of the tremor spectrum of each of the limb segments is expressed relative to that measured from the finger (taken as 100%), with the exception of the finger for the same subject. As shown in Fig. 4, the total power of the tremor spectrum was different for each of the limb segments. The finger tremor exhibited the largest total power among the four different limb segments. The total power of the hand tremor was half that of the finger tremor. Although the mass of the forearm was lighter than that of the upper limb, the total power of the forearm tremor was smaller than that of the upper limb tremor. During the measurement of forearm tremor, the movement of the forearm was restricted due to the placement of the elbow and a part of the forearm on the board (mechanical ground; Fig. 1c). Therefore, the vibration of the forearm in the vertical direction was reduced. On the other hand, for the limb segments except for the forearm, the movement of the limb segment was not restricted by its posture during the measurement.

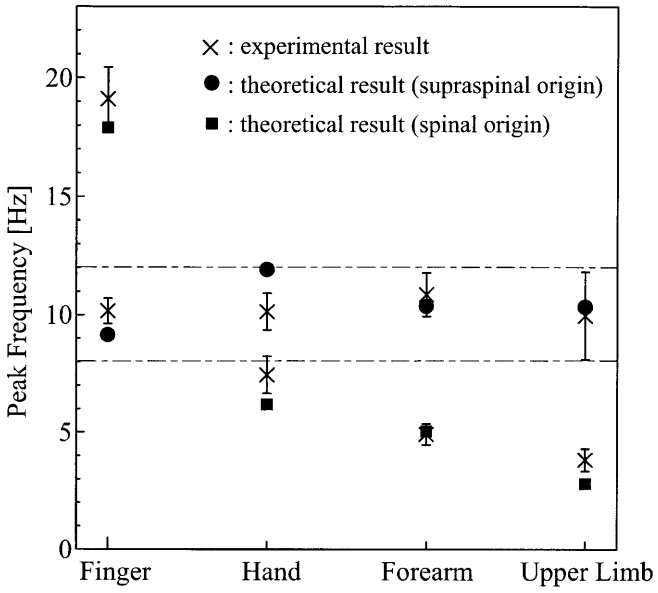

Fig. 3 Dependence of the two peak frequencies in the tremor spectrum on the limb segment: theoretical and experimental results are shown. The *crosses* indicate experimental results. *Closed circles* and *closed squares* indicate peak frequencies of the supraspinal component of the tremor and that of spinal origin predicted by the tremor model, respectively. The zone delineated by the *dotted line* shows the range of α rhythm from 8 to 12 Hz

Theoretical study of the tremor of four upper limb segments

Methods

Development of the tremor model

The tremor model has been developed to explain the peak frequencies and the amplitudes in the tremor spectrum for the four kinds of upper limb segments. As shown in Fig. 5, the tremor model is composed of five subsystems:

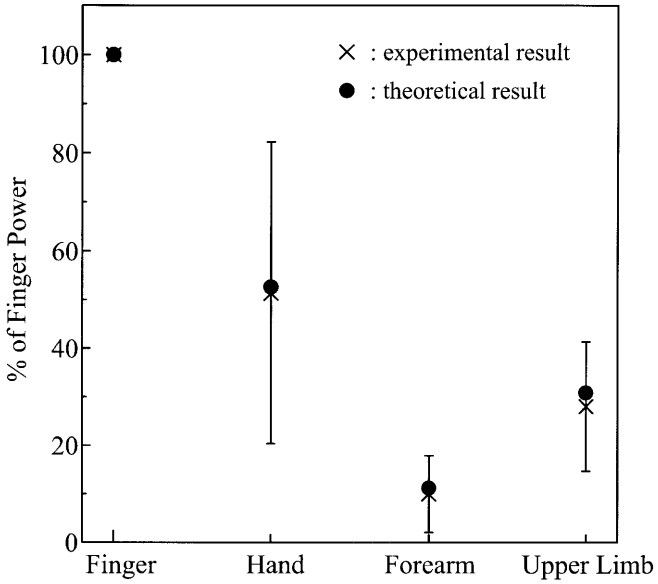

Fig. 4 Dependence of relative power on the limb segment (i.e., relative value of the total power of tremor spectrum): theoretical and experimental results are shown. The *crosses* and *closed circles* indicate experimental results and theoretical values predicted by the tremor model, respectively. Total power for the finger tremor for each subject was taken to be 100%, and the relative values of total powers for all subjects are averaged. The experimental results of mean (SD) of total power for finger tremor, hand tremor, forearm tremor, and upper limb tremor are 2.02 (1.40) mV^2 (i.e., 100%), 0.95 (0.66) mV^2, 0.17 (0.15) mV^2, and 0.45 (0.16) mV^2, respectively. The theoretical value is the amplitude evaluated as $(\theta_0 f^2_{peak})_{spinal} + (\theta_0 f^2_{peak})_{supraspinal}$. The theoretical values for the finger, hand, forearm, and upper limb are $1.07\times10^5\cdot s^{-2}$, $5.62\times10^4\cdot s^{-2}$, $1.20\times10^3\cdot s^{-2}$, and $3.30\times10^3\cdot s^{-2}$, respectively

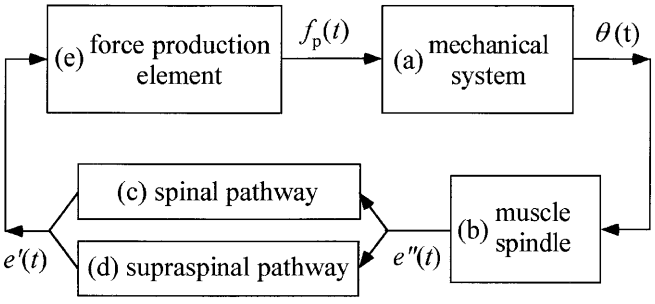

Fig. 5 Block diagram of tremor model of an upper limb segment. The model consists of a mechanical system of limb segment and muscles (*a*), muscle spindle (*b*), spinal pathway (*c*), supraspinal pathway (*d*), and a force production element (*e*). The system (e) is the element of the force produced by the muscular contraction which was driven by the signal of the efferent nerve via two pathways (c) and (d). The displacement of angle of limb segment $\theta(t)$ corresponds to the tremor

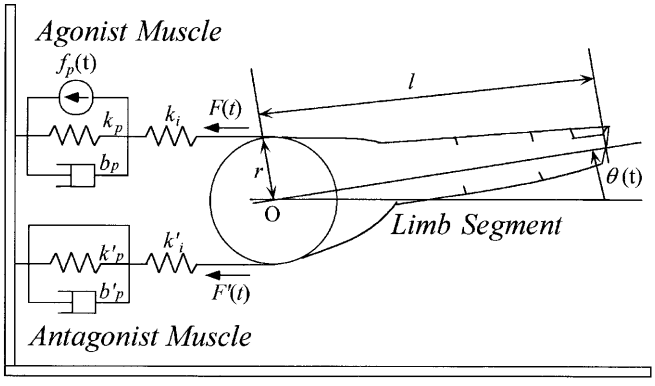

Fig. 6 Mechanical system of limb segment and muscles. This figure illustrates the system for a finger. The limb segment is moved to a displacement of angle $\theta(t)$ by the agonist muscle (k_i, k_p, b_p) and antagonist muscle (k'_i, k'_p, b'_p). k_i, k_p, and b_p are the series elastic element, parallel elastic element, and viscous element of the agonist muscle, respectively. k'_i, k'_p and b'_p are the series elastic element, parallel elastic element, and viscous element of the antagonist muscle, respectively. $f_p(t)$ denotes the force produced by force production element

(a) the mechanical system of the limb segment and the muscles, (b) the muscle spindle, (c) the spinal pathway, (d) the supraspinal pathway, and (e) the active element (i.e., the force production element). The development of the model for finger tremor has been described previously (Miao and Sakamoto 1995b; Arihara and Sakamoto 1999b). The formulation of the subsystems and the derivation of the equations for the model in the closed loop system are summarized as follows.

Figure 6 illustrates the mechanical system of the limb segment and the muscles. The mechanical system of the limb segment is assumed to be a simple system that can be described by a linear second-order equation. The limb segment is moved to a displacement of angle $\theta(t)$ by an external torque produced by the agonist and the antagonist muscles, $F(t)\cdot r - F'(t)\cdot r$. $F(t)$ and $F'(t)$ are the forces of the agonist and the antagonist muscles, respectively, shown in Fig. 6. The term r denotes the radius of the limb segment. It is assumed that the radius of the limb segment is the same for both muscles. The equation of the motion for the mechanical system is formulated:

$$F(t)\cdot r - F'(t)\cdot r = I\frac{d^2\theta(t)}{dt^2} + C_e\frac{d\theta(t)}{dt} + K_e\theta(t) + mg\left(\frac{l}{2}\right) \quad (1)$$

where I, C_e, and K_e are the moment of inertia, the joint friction, and the joint stiffness of the limb segment, respectively. The term $mg(l/2)$ is the gravitational moment of the limb segment; m, l, and g are the mass and length of the limb segment, and the acceleration of gravity (i.e., 9.8 m/s^2), respectively. Equation 1 may be reformulated:

$$F(t) - F'(t) = \frac{I}{r}\left(\frac{d^2\theta(t)}{dt^2} + J_e\frac{d\theta(t)}{dt} + \omega_e^2\theta(t) + \frac{mgl}{2I}\right) \quad (2)$$

where $J_e = C_e/I$ and $\omega_e^2 = K_e/I$.

The mechanical system of the agonist and the antagonist muscles has been considered to be a second-order linear system (Miao and Sakamoto 1995b; Sakamoto et al. 1998). The second-order linear system for the muscles is quantified by the lumped-parameter model (Winters and Stark 1987; Zajac 1989). The ag-

onist muscle consists of the series (k_i) and the parallel (k_p) elastic elements, the viscous element b_p, and the force production element $f_p(t)$. The relationship between the force of the agonist muscle $F(t)$ and the change in muscle length, $X(t)=r\theta(t)$, may be quantified as:

$$\left(\frac{d}{dt}+\alpha\right)F(t)=\frac{k_i}{b_p}\left[f_p(t)-\left(b_p\frac{d}{dt}+k_p\right)r\theta(t)\right] \tag{3}$$

where $\alpha=(k_i+k_p)/b_p$. The antagonist muscle is also quantified by the series (k_i') and parallel (k_p') elastic elements, and the viscous element b_p'. The relationship between the force of the antagonist muscle $F'(t)$ and the change of the muscle length $X'(t)=-r\theta(t)$ is derived as follows:

$$\left(\frac{d}{dt}+\alpha'\right)F'(t)=\frac{k_i'}{b_p'}\left[+\left(b_p'\frac{d}{dt}+k_p'\right)r\theta(t)\right] \tag{4}$$

where $\alpha'=(k_i'+k_p')/b_p'$. The force production element of the antagonist muscle, $f_p'(t)$, is omitted because the muscle does not contract against gravity.

The relationship between the change in muscle length and the modulation of the discharge rate of the muscle spindle is quantified by the linear function in terms of the displacement and the velocity (i.e., the transducer-encoder process; Hasan 1983). The transducer-encoder process is expanded by the muscle spindle model proposed by Zahalak and Cannon (1983). In their study, the property of the muscle spindle was investigated by forced oscillation tests (Cannon and Zahalak 1981). They concluded that the muscle spindle detected the acceleration component of the movement of the muscle other than the displacement and the velocity components. Therefore, the discharge rate of the muscle spindle, $e''(t)$, is obtained as follows:

$$\begin{aligned}e''(t)&=H_d\left[X(t)+T_m\frac{dX(t)}{dt}+a_2\frac{d^2X(t)}{dt^2}\right]\\&=H_a\left[\theta(t)+T_m\frac{d\theta(t)}{dt}+a_2\frac{d^2\theta(t)}{dt^2}\right]\end{aligned} \tag{5}$$

where H_d is the sensitivity of the muscle spindle for the muscle displacement, and H_d is treated as a proportional constant between $e''(t)$ and the second order differential equation of $X(t)$. $X(t)=r\theta(t)$ and $H_a=rH_d$ are used; T_m and a_2 denote the velocity and the acceleration sensitivities of the muscle spindle, respectively.

As shown in Fig. 7, the nervous system consists of two reflex pathways, the spinal pathway and the supraspinal pathway (Watanabe and Saito 1984; Miao and Sakamoto 1995b). The afferent signal from the muscle spindle, $e''(t)$, is transmitted to both the spinal system and the supraspinal system. The efferent signal from the nervous system, $e'(t)$, is represented by the sum of the signals from the spinal system, $e_1'(t)$, and the supraspinal system, $e_2'(t)$:

$$\begin{aligned}e'(t)&=e_1''(t)+e_2''(t)\\&=H_1\left[\theta(t-\tau_1)+T_m\frac{d\theta(t-\tau_1)}{dt}+a_2\frac{d^2\theta(t-\tau_1)}{dt^2}\right]\\&\quad+H_2\left[\theta(t-\tau_2)+T_m\frac{d\theta(t-\tau_2)}{dt}+a_2\frac{d^2\theta(t-\tau_2)}{dt^2}\right]\\&=H_1\left\{\left[\theta(t-\tau_1)+T_m\frac{d\theta(t-\tau_1)}{dt}+a_2\frac{d^2\theta(t-\tau_1)}{dt^2}\right]\right.\\&\quad\left.+h\left[\theta(t-\tau_2)+T_m\frac{d\theta(t-\tau_2)}{dt}+a_2\frac{d^2\theta(t-\tau_2)}{dt^2}\right]\right\}\end{aligned} \tag{6}$$

where τ_1 and τ_2 denote the time delays in the spinal and the supraspinal pathways in the nervous system. H_1 and H_2 indicate the gains in the spinal and the supraspinal systems, respectively. The gain ratio is defined as $h=H_2/H_1$ (gain in the supraspinal system/gain in the spinal system). In Eq. 6, the relationship between the afferent signal from the muscle spindle, $e''(t)$, and the efferent signal, $e'(t)$, is linear. The gain ratio h is the same, regardless of the limb segment under investigation.

The efferent signal from the nervous system, $e'(t)$, is converted to the isometric force of the muscle, $f_p(t)$, in the force production element. The isometric force is quantified by a sigmoid function of $e'(t)$ (Stein and Oðuztöreli 1976):

$$f_p(t)=\frac{S_b}{2}\tanh\left(\frac{S_a e'(t)}{2}\right) \tag{7}$$

where $S_a=5.0\times10^{-3}$ m/pulses/s (m/pps). S_b represents the maximum force produced by the force production element. The details are described in the section headed "Parameter setting".

Substituting Eqs. 3 and 4 divided by $[(d/dt)+\alpha]$ or $[(d/dt)+\alpha']$ into Eq. 2, we obtain:

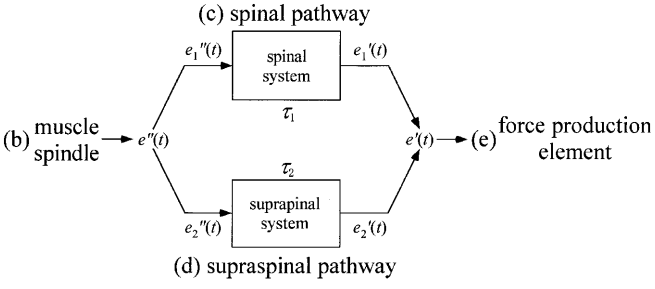

Fig. 7 Reflex pathways controlled by four subsystems in the nervous system. The afferent signal from the muscle spindle (*b*), $e''(t)$, is transmitted to the spinal system (*c*) and the supraspinal system (*d*). The efferent signal from the nervous system, $e'(t)$, is sent to the force production element (*e*). τ_1 and τ_2 denote time delays in the spinal and supraspinal pathways, respectively

$$\frac{k_i}{b_p}\left[f_p(t)-\left(b_p\frac{d}{dt}+k_p\right)r\theta(t)\right]\Big/\left(\frac{d}{dt}+\alpha\right)$$
$$-\frac{k_i'}{b_p'}\left[\left(b_p'\frac{d}{dt}+k_p'\right)r\theta(t)\right]\Big/\left(\frac{d}{dt}+\alpha'\right)$$
$$=\frac{I}{r}\left(\frac{d^2}{dt^2}+J_e\frac{d}{dt}+\omega_e^2+\frac{mgl}{2I}\right)\theta(t) \quad (8)$$

Both sides of Eq. 8 are multiplied by $\left(\frac{d}{dt}+\alpha\right)\left(\frac{d}{dt}+\alpha'\right)$, and Eq. 7 (which describes $f_p(t)$) is substituted into Eq. 8:

$$\frac{k_i}{b_p}\left(\frac{d}{dt}+\alpha'\right)\left[\frac{S_b}{2}\tanh\left(\frac{S_a e'(t)}{2}\right)-\left(b_p\frac{d}{dt}+k_p\right)r\theta(t)\right]$$
$$-\frac{k_i'}{b_p'}\left(\frac{d}{dt}+\alpha\right)\left[\left(b_p'\frac{d}{dt}+k_p'\right)r\theta(t)\right]$$
$$=\frac{I}{r}\left(\frac{d}{dt}+\alpha\right)\left(\frac{d}{dt}+\alpha'\right)\left(\frac{d^2}{dt^2}+J_e\frac{d}{dt}+\omega_e^2+\frac{mgl}{2I}\right)\theta(t) \quad (9)$$

A nonlinear closed equation for the tremor model is obtained from Eq. 9:

$$A\left(\frac{d}{dt}+\alpha'\right)\frac{S_b}{2}\tanh\left(\frac{S_a e'(t)}{2}\right)$$
$$=\left(\frac{d}{dt}+\alpha\right)\left(\frac{d}{dt}+\alpha'\right)\left(\frac{d^2}{dt^2}+J_e\frac{d}{dt}+\omega_e^2+\frac{mgl}{2I}\right)\theta(t)$$
$$+\left(\frac{d}{dt}+\alpha'\right)\left(B\frac{d}{dt}+D\right)\theta(t)+\left(\frac{d}{dt}+\alpha\right)\left(B'\frac{d}{dt}+D'\right)\theta(t) \quad (10)$$

where

$$e'(t)=H_1\left[\left(1+T_m\frac{d}{dt}+a_2\frac{d^2}{dt^2}\right)\theta(t-\tau_1)\right.$$
$$\left.+h\left(1+T_m\frac{d}{dt}+a_2\frac{d^2}{dt^2}\right)\theta(t-\tau_2)\right] \quad (11)$$

and $A=rk_i/Ib_p$, $B=r^2k_i/I$, $D=Bk_p/b_p$, $B'=r^2k_i'/I$, and $D'=B'k_p'/b_p'$.

Since the tremor is a periodic oscillation, the displacement of the angle of the limb segment $\theta(t)$ is expressed by $\theta(t)=\theta_0\exp(j\omega t)$, where θ_0 and ω represent the displacement and the angular frequency of the oscillation, respectively. The angular frequency is calculated by $\omega=2\pi f$, where f is the frequency of the oscillation. Substituting this relationship into Eq. 11, the efferent signal from the nervous system, $e'(t)$, is obtained:

$$e'(t)=H_1(1+jT_m\omega-a_2\omega^2)\cdot(1+he^{-j\omega(\tau_2-\tau_1)})$$
$$\cdot e^{-j\omega\tau_1}\cdot\theta_0 e^{j\omega t}=p\theta_0 e^{j(\omega t+\psi)} \quad (12)$$

where j is an imaginary number (i.e., root(–1)), and

$$p=H_1\left\{\left[(1-a_2\omega^2)^2+(T_m\omega)^2\right]\right.$$
$$\left.\times\left[(h\sin(\omega\Delta\tau))^2+(1+h\cos(\omega\Delta\tau))^2\right]\right\}^{1/2}$$
$$\psi=\pi-\omega\tau_1+\tan^{-1}\frac{T_m\omega}{1-a_2\omega^2}-\tan^{-1}\frac{h\sin(\omega\Delta\tau)}{1+h\cos(\omega\Delta\tau)} \quad (13)$$

where $\Delta\tau=\tau_2-\tau_1$. Although the force production element is quantified by a nonlinear function, as shown in Eq. 7, the function is approximated as the fundamental harmonic:

$$\frac{S_b}{2}\tanh\left(\frac{S_a e'(t)}{2}\right)=E_1e^{j(\omega t+\psi)}+\ldots$$
$$\cong E_1e^{j(\omega t+\psi)} \quad (14)$$

The amplitude of the fundamental harmonic E_1 is obtained by the Fourier expansion theory (Sakamoto et al. 1998; Arihara and Sakamoto 1999b):

$$E_1=\frac{1}{\pi}\int_{-\pi}^{\pi}\frac{S_b}{2}\tanh\left(\frac{S_a\mathrm{Re}\{e'(t)\}}{2}\right)\cos\xi d\xi$$
$$=\frac{1}{\pi}\int_{-\pi}^{\pi}\frac{S_b}{2}\tanh\left(\frac{S_a p\theta_0\cos\xi}{2}\right)\cos\xi d\xi \quad (15)$$

where Re denotes a real number and $\psi=\xi t+\psi$. Substituting Eqs. 12, 14 and 15 into Eq. 10, a complex algebra equation for the tremor model is obtained:

$$\frac{1}{\pi}\int_{-\pi}^{\pi}\frac{S_b}{2}\tanh\left(\frac{S_a p\theta_0\cos\xi}{2}\right)\cos\xi d\xi\cdot e^{j\psi}$$
$$=\theta_0\cdot\frac{1}{A}(j\omega+\alpha)\left[\left(J_e j\omega+\Delta\omega^2+\frac{mgl}{2I}\right)\right.$$
$$\left.+\frac{Bj\omega+D}{j\omega+\alpha}+\frac{B'j\omega+D'}{j\omega+\alpha'}\right] \quad (16)$$

where $\Delta\omega^2=\omega_e^2-\omega^2$.

The left hand side of Eq. 16 is called the "nervous reflex term" (NRT), while the right side is termed the "muscle mechanical term" (MMT). Both terms are a function of the frequency ($f=\omega/2\pi$) and the displacement (θ_0) of the oscillation of the limb segment $\theta(t)$. The NRT has a phase ψ and a magnitude:

$$\left|\frac{1}{\pi}\int_{-\pi}^{\pi}\frac{S_b}{2}\tanh\left(\frac{S_a p\theta_0\cos\xi}{2}\right)\cos\xi d\xi\right| \quad (17)$$

The MMT also has a phase and a magnitude. The intersection point between the phase of NRT and the phase of MMT corresponds to the solution of the complex algebra equation for the tremor model. The peak fre-

quency of the tremor spectrum (f_{peak}) is obtained from the frequency at the intersection point. The amplitude of the tremor is also evaluated by Eq. 16. The displacement component of the tremor (θ_0) is obtained from the intersection point between the magnitude of NRT and the magnitude of MMT. The displacement component is converted to the amplitude of the acceleration component by $\theta_0 f_{peak}^2$ (Arihara and Sakamoto 1999b).

Parameter setting

In this study, the mechanism underlying the tremor is treated by a simple mechanical model as the first step toward simulation research. The limb segment is assumed to be a rigid, cylindrical body with a length l, a radius r, and a mass m (Fig. 6). The moment of inertia (I) of the limb segment may be obtained as follows:

$$I = \frac{1}{3} m l^2 \tag{18}$$

The mass, the length, and the radius of the limb segments are listed in Table 1. It is assumed that the viscoelastic elements of the muscle are the sum of those of the muscle fibers constituting the muscle. If the shape of the muscle is a massed cylinder with a cross-sectional area (S), where $S = \pi r^2$, the viscoelastic elements of the agonist and the antagonist muscles are proportional to the cross-sectional area: $k_i = k_{i0} \times S$, $k'_i = k'_{i0} \times S$; $k_p = k_{p0} \times S$, $k'_p = k'_{p0} \times S$; $b_p = b_{p0} \times S$, $b'_p = b'_{p0} \times S$; where k_{i0}, k_{p0}, b_{p0}, k'_{i0}, k'_{p0} and b'_{p0} are the values of the viscoelastic elements per unit cross-sectional area. The estimations of the parameters of the viscoelastic elements have been studied for a single muscle by various authors (Bawa et al. 1976; Oðuztöreli and Stein 1976). The parameters of the viscoelastic elements for two muscles (i.e., antagonistic muscles) have been proposed by Oðuztöreli and Stein (1982, 1990). The values of the viscoelastic elements were modified by research using the model of the finger tremor (Sakamoto et al. 1998). In the study of Sakamoto et al. (1998) the simulation results were in good agreement with the experimental results. In the present study, the shape of the limb segment is taken as a cylinder. The cross-sectional area of the cylinder is πr^2, r being the radius of the cylinder. The values of the viscoelastic elements per unit sectional area for the muscles of the four limb segments are quantified by the values of the viscoelastic elements for the finger tremor and the cross-sectional area of the muscle. The characteristics of the muscles for the different limb segments are considered to be uniform, as in the simple mechanical model: $k_{i0} = 9.0 \times 10^6\ \mathrm{N/m^3}$, $k'_{i0} = 1.8 \times 10^7\ \mathrm{N/m^3}$; $k_{p0} = 3.6 \times 10^6\ \mathrm{N/m^3}$, $k'_{p0} = 7.2 \times 10^6\ \mathrm{N/m^3}$; $b_{p0} = 2.0 \times 10^5\ \mathrm{Ns/m}]3$, $b'_{p0} = 2.0 \times 10^5\ \mathrm{Ns/m^3}$, where the units N, s, and m denote Newton, second, and meter.

In the present model, the muscle producing the mechanical vibration of the limb segment is the agonist muscle, while the antagonist muscle does not produce the force because the finger is pulled down by gravity (Fig. 6). The values of the viscoelastic elements used are those that Oðuztöreli and Stein (1982, 1990) obtained for the model of two muscles. The joint properties for the respective segments in the upper limb are considered to be the same because the joints are the fulcrums, as shown in Fig. 6. The joints have no connection with the calculation of the mechanical property of the limb segment. The magnitudes of the parameters for the agonist and the antagonist muscles are set uniformly, but the cross-sectional areas of the limb segments are different. Therefore, the parameters of the viscoelastic elements depend upon the scale of the limb segment.

The joint stiffness of the limb segment, K_e, in Eq. 1 is the sum of the values of the series elastic elements of the agonist and the antagonist muscles (Lan and Crago 1994):

$$K_e = r^2(k_i + k'_i) \tag{19}$$

The value K_e is evaluated in Eq. 10 as $\omega_e^2 = K_e/I$. In Eq. 19, the passive muscle stiffness of k_p and k'_p is ignored since the sum of the values is smaller by one-third than the sum of the other muscle stiffness values (i.e., k_i and k'_i). Moreover, Lan and Crago (1994) evaluated only

Table 1 Mass (m), length (l), and radius (r) of four different upper limb segments

Limb segment	m (kg)	l (m)	r (m)
Finger	0.023	0.082	0.010
Hand	0.550	0.190	0.025
Forearm	1.440	0.450	0.038
Upper limb	3.100	0.800	0.045

Table 2 Parameters for the muscle spindle, two reflex pathways, and the force production element of four different upper limb segments: velocity (T_m) and acceleration (a_2) sensitivities of the muscle spindle, time delays in the spinal pathway (τ_1) and the supraspinal pathway (τ_2), and scaling parameter for the force production element (β)

Limb segment	Sensitivity of muscle spindle		Time delay in reflex pathway		Force production element
	Velocity T_m (s)	Acceleration a_2 (s^2)	Spinal τ_1 (s)	Supraspinal τ_2 (s)	Scaling parameter β
Finger	1.50×10^{-2}	1.00×10^{-3}	4.10×10^{-2}	8.10×10^{-2}	1.00
Hand	1.50×10^{-2}	2.00×10^{-4}	3.60×10^{-2}	8.80×10^{-2}	0.60
Forearm	1.50×10^{-2}	1.00×10^{-4}	3.10×10^{-2}	9.10×10^{-2}	0.10
Upper limb	1.50×10^{-2}	1.00×10^{-4}	3.10×10^{-2}	9.10×10^{-2}	0.50

the muscle stiffness of k_i and k'_i in the control of the voluntary movement and did not considered the muscle stiffness of k_p and k'_p. The joint friction of the limb segment C_e in Eq. 1 is a function of the square root of the joint stiffness K_e (Kearney and Hunter 1990):

$$C_e = C_0 + \gamma_1 \sqrt{K_e} \tag{20}$$

where $C_0 = 1.225\times10^{-3}$ sNm and $\gamma_1 = 1.5\times10^{-4}$ s(Nm)$^{1/2}$. The value C_e is evaluated in Eq. 10 as $J_e = C_e/I$.

The velocity sensitivity T_m and the acceleration sensitivity a_2 in the muscle spindle are listed in Table 2. For the finger tremor, these sensitivities in the muscle spindle are determined to be the same as in the model proposed by Sakamoto et al. (1998). In their model, these values were determined by the experimental findings of Zahalak and Cannon (1983). As shown in Fig. 3, the frequency of the finger tremor is higher than those of the forearm tremor and the upper limb tremor. This result means that the movement of a limb segment with a light mass, such as the finger, is faster than the movement of the limb segment with a heavy mass, such as the upper limb. When the faster movement of the limb segment is controlled by the nervous system, the acceleration component of the movement is more important than the displacement and velocity components in the calculation of the amplitude of the tremor wave. This is thought to be due to the following evaluation of the tremor wave.

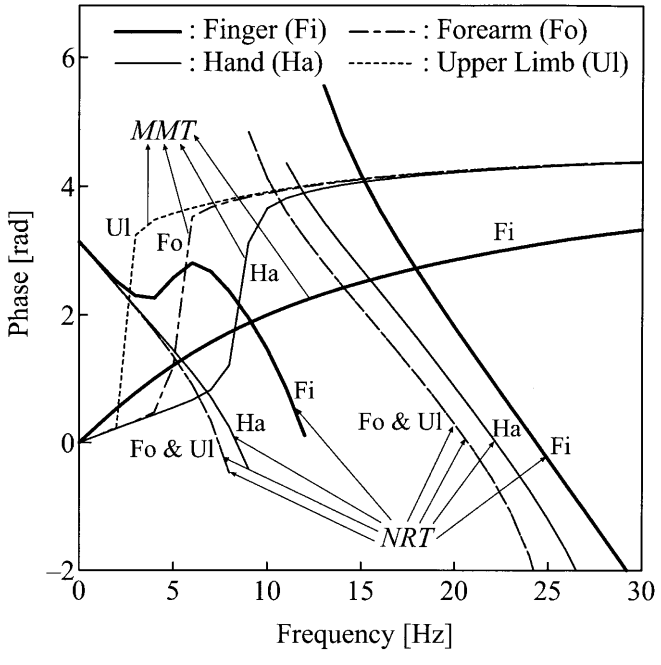

Fig. 8 Phase curves of the "nervous reflex term" (*NRT*) and the "muscle mechanical term"(*MMT*) for four different upper limb segments. *Thick* and *thin solid lines* denote phase curves of NRT and MMT for the finger (*Fi*) and hand (*Ha*), respectively. *Chain* and *dotted lines* represent the phase curves of NRT and MMT for the forearm (*Fo*) and upper limb (*Ul*), respectively. Frequencies at interaction points between phase curves of NRT and MMT correspond to peak frequencies at two prominent peaks of the tremor spectrum

When a tremor of any limb segment is detected as the displacement component, the mechanical vibration (y) is represented as $y = A\sin\omega t$, where A is the component of the displacement and ω is the angular frequency of the mechanical vibration. The velocity and acceleration components, $\dot{y}$ and $\ddot{y}$, respectively, are obtained as $\dot{y} = \omega A\cos\omega t$ and $\ddot{y} = -\omega^2 A\sin\omega t = \omega^2(-y)$, respectively. Therefore, the amplitude of the acceleration component is the largest of the three components. The results shown in Figs. 2(b) and 4 show that the total power of the finger tremor is larger than that of the hand tremor. The total power of the hand tremor is also larger than that of the forearm tremor. These results indicate that the amplitude of the acceleration component for the limb segment with the smaller mass is larger than that for the limb segments with the heavier mass. This experimental fact is reflected by the variation of the acceleration sensitivity a_2, as shown in Table 2. The velocity sensitivity does not change with the mass of the limb segment, that is, $T_m = 1.5\times10^{-2}$ (s).

As listed in Table 2, the time delay in the spinal pathway, τ_1, is shortened with the narrowing of the distance between the limb segment and the spinal cord, while the time delay in the supraspinal pathway, τ_2, is prolonged. As for the parameter setting of τ_1, Lenz et al. (1983) found experimentally that the value of τ_1 for the limb segments in the monkey was smaller when the limb segment was closer to the spinal cord. That tendency is the same as our parameter setting of τ_1. It is considered that the value of τ_2 is different to that of τ_1 because the supraspinal system is under the influence of the lower nervous system (i.e., the neuromuscular system under the control of the spinal system). That is, the value of τ_2 does not depend upon the location of the limb segment.

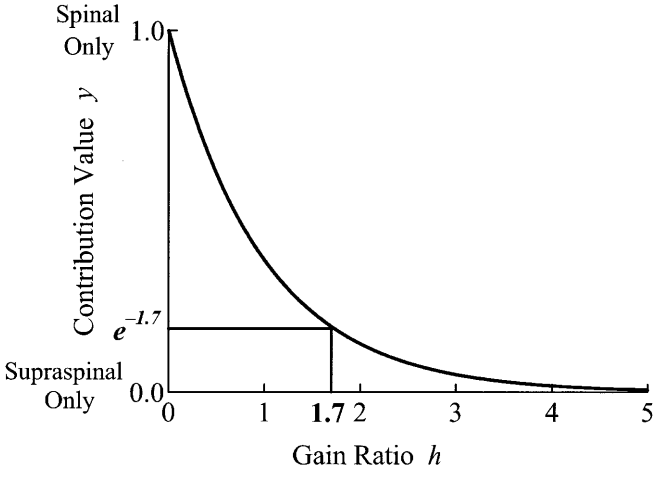

Fig. 9 Relationship between the value of the gain ratio h and the contribution value y by the nervous systems (i.e., the spinal and supraspinal systems). The value of the ordinate indicates the contribution of the spinal and supraspinal systems. The contribution value of unity indicates the existence of a spinal system only, while the value of zero denotes the existence of a supraspinal system only. The relationship is given by the function $y = e^{-h}$. In this study, the case of $h = 1.7$ is used; $y = e^{-1.7}$

In the study presented here, it is estimated that the value of τ_2 depends upon the mass of the limb segment because the supraspinal signal (i.e., the voluntary command) plays a role in maintaining or moving the limb segment. The gain in the spinal system is determined as $H_1 = 3.0\times10^4$ pps/m. This value was used in the model proposed by Sakamoto et al. (1998), who calculated it using the experimental findings of Zahalak and Cannon (1983). The gain ratio is determined as $h = 1.7$ (Miao and Sakamoto 1995b; Sakamoto et al. 1998).

Since the force produced by the force production element $f_p(t)$ depends upon the limb segment under study, the maximum force produced by the force production element, S_b, is proportional to the cross-sectional area of the muscle, $S = \pi r^2$: $S_b = \beta S_{b0} S$, where $S_{b0} = 1.0\times10^7$ (N/m^2). β is the scaling parameter for S_b, and the value of β is determined to coincide with the experimental data (i.e., the amplitude) as listed in Table 2.

Results

Figure 8 shows the phase curves of NRT and MMT for the four limb segments studied. The frequency at the intersection point between the phase curves of NRT and MMT corresponds to the peak frequency of the tremor spectrum. As shown in Fig. 8, there exist two intersection points between the phase curves of NRT and MMT for all the limb segments, suggesting that there are two frequency components in the tremor of the four different limb segments.

The tremor model was analyzed under the various values of the gain ratio h to investigate whether the two frequency components are attributable to the spinal system or to the supraspinal system (Sakamoto et al. 1998). Figure 9 shows the relationship between the value of the gain ratio h and the contribution of the nervous systems. If only the spinal system contributes (i.e., $h = 0.0$), the tremor has a single frequency component. When the gain ratio h increases and becomes $h > 1.0$, the tremor has two frequency components. This result indicates that the frequency component for which $h \gg 1.0$ originates mostly from the supraspinal system. The other frequency component is generated from the spinal system. On the basis of this analysis, one of the two frequency components has been identified as being of spinal origin, and the other as the component of supraspinal origin.

Figure 3 shows a comparison of the frequencies of the two frequency components predicted by the tremor model and obtained by the experimental results. The theoretical values of the peak frequencies (closed circles and closed squares) agree well with the experimental results (crosses). The component of supraspinal origin exists in the range 8–12 Hz (Sakamoto et al. 1993). The peak frequency of this component does not depend upon the mass of the limb segment. On the other hand, the peak frequency of the component of spinal origin decreases with the increase in the mass of the limb segment. As shown in Fig. 8, the peak frequency of this component is determined by the frequency at which the phase of MMT increases drastically for the different limb segments. These results imply that the peak frequency of the spinal component is determined by the mechanical system of the limb segment. The peak frequency of this component is about 20 Hz for the finger tremor, but it decreases to about 4 Hz for the upper limb tremor. When the mass of the limb segment is heavier than the finger, the peak frequency due to the spinal component is lower than that of the supraspinal component, as shown in Fig. 3.

The amplitude of the acceleration component of the tremor can be estimated by the tremor model. The tremor model predicts the amplitude of the spinal component, $(\theta_0 f_{peak}^2)_{spinal}$, and that of the supraspinal component, $(\theta_0 f_{peak}^2)_{supraspinal}$. Since the tremor is composed of the two frequency components, the amplitude of the acceleration component of the tremor is estimated by the sum of the amplitude of the spinal component and the supraspinal component (i.e., $(\theta_0 f_{peak}^2)_{spinal} + (\theta_0 f_{peak}^2)_{supraspinal}$). The values of θ_0 (radian unit) for the limb segments may be calculated using Eq. 16 as follows: The values are 18.3 rad (finger), 20.5 rad (hand), 11.4 rad (forearm), and 104.2 rad (upper limb). Figure 4 shows the relative variation in the amplitude of the acceleration component of the tremor predicted by the tremor model. The amplitude of the acceleration component of the tremor corresponds to the total power of the tremor spectrum obtained in the experimental study. The theoretical value of the amplitude of the acceleration component predicted by the tremor model (closed circles) agrees well with the experimental results (crosses). The agreement of the theoretical and the experimental results is achieved by the scaling parameter of the force production element, β, as listed in Table 2. The scaling parameter, β, is determined by the conditions used during the measurement of the tremor. For example, the elbow and a part of the forearm was resting on the board during the measurement of the forearm tremor (Fig. 1c). The movement of the forearm in the vertical direction (i.e., the tremor) is thus restricted. Therefore, the β is decreased to 0.10 for the forearm tremor.

Discussion

An acceleration signal of the tremor for the four different upper limb segments studied (i.e., finger, hand, forearm, and upper limb) was measured with the aid of an acceleration sensor. Since two prominent peaks appeared in the power spectrum of the tremor for all the limb segments (Fig. 2b), the tremor for the four different limb segments must be composed of two frequency components. Arihara and Sakamoto (1999a) measured the tremor in the finger under conditions of

adding weight loads onto the finger. The frequency of the lower frequency component (8–12 Hz) did not change in spite of the addition of the weight load, while the higher-frequency component was shifted to the lower frequency domain by the addition of the weight load. In this study, the two frequency components of the tremor observed for the four limb segments studied showed a similar variation.

It is thought that the tremor originates from the activity of the nervous system. This assumption has been supported by surface electromyogram (EMG) experiments in which a tremor was measured (Elble and Randall 1978; Matthews and Muir 1980; Arihara and Sakamoto 1999a; Halliday et al. 1999). In these studies, the relationship between the tremor and the EMG was investigated. The coherence spectrum (the correlation in the frequency domain) exhibited significant peaks at about 10 Hz and 20 Hz. These results verified that the two frequency components of the tremor were produced by the nervous system. Watanabe and Saito (1984) and Sakamoto et al. (1993) proposed that two parts of the nervous system, the spinal system and the supraspinal system, give rise to the tremor. The experimental and theoretical analyses of the tremor model for the limb segments examined in the present study verify this hypothesis. The two frequency components appear in the tremor for all four of the different limb segments (Figs. 2(b), 3, 8). The appearance of these two frequency components may be explained by the assumption of the existence of two reflex pathways in the nervous system (Fig. 7). Lippold (1970) suggested that the servo-loop in the stretch reflex system, which occurs via the spinal cord, gives rise to the tremor. Although that hypothesis was partly true, other researchers have pointed out that the servo-loop in the spinal system was not unique to the tremor. In addition to the spinal system, the tremor was also attributed to the supraspinal system, which involves the cerebral cortex and the thalamus (Elble and Koller 1990; Findley and Koller 1995). The involvement of the two nervous systems in the tremor concurs with our assumption for the tremor model. The two reflex pathways in the nervous system are recognized as the spinal system and the supraspinal system. The two frequency components of the tremor are identified as the components that are of spinal origin and supraspinal origin, respectively, by the analysis of the tremor model under the various values of the gain ratio h (i.e., ratio of the gain in the supraspinal system to the gain in the spinal system).

The theoretical results show that the frequency of the spinal component decreases with increases in the mass of the limb segment, while the frequency of the supraspinal component (8–12 Hz) is independent of the mass of the limb segment. It is thought that the frequency of the spinal component depends upon the mass of the limb segment because the spinal system produces the tremor (a mechanical vibration) due to the mechanical system of the limb segment. On the other hand, the supraspinal system plays a role in the maintenance of the posture of the limb segment. According to studies of pathological tremors, like that experienced by sufferers of Parkinson's disease, and animal experiments, it is considered that the activity in the supraspinal system is related to the generation of the tremor (Elble et al. 1984; Köster et al. 1998). The structure and activity of the supraspinal system is complex, and the motoneurons in the spinal cord are controlled by the activity of the supraspinal system (Elble and Koller 1990; Findley and Koller 1995; Elble 1996). Therefore, the resulting indirect effect of the supraspinal system on the spinal system is thought to produce the constant frequency that determines the frequency of the α rhythm, 8–12 Hz, irrespective of the mass of the limb segment.

The behavior of both the spinal and the supraspinal systems has also been verified by experiments using both immersion of the finger in water and the addition of weight loads onto the finger (Sakamoto et al. 1993). When the finger was immersed in water, the power spectrum of the finger tremor exhibited a larger decrease in the higher-frequency domain, at around 20 Hz, than in the lower-frequency domain, at around 10 Hz. Sakamoto et al. (1993) suggested that the activity of thespinal system was reduced more than the activity of the supraspinal system under conditions of immersion of the finger in water, chiefly due to the buoyancy afforded by water. This result indicated that the higher-frequency component of the tremor originated from the spinal system. The origin of the lower-frequency component of the finger tremor was shown by the experiments using weight loading of the finger. When the weight load was increased, the amplitude (i.e., the power spectrum) in the frequency range at around 10 Hz increased markedly, but the amplitude in the higher frequency at around 20 Hz did not show a great increase. The increase in the amplitude of the lower frequency peak was considered to be caused by the effect of voluntary effort against the increasing weight load. Our assumption regarding the origin of the tremor is supported by the finger-immersion and weight-load experiments and by the theoretical model described in the study reported here.

The agreement between the experimental and the theoretical results of the present study regarding the mechanism of the tremor suggests the following contributions. The evaluation of the characteristics of the tremor (i.e., the frequency and the amplitude) that are of spinal origin could represent the function of the mechanical system (e.g., the function of maintaining posture) for normal subjects. As for patients with a neuromuscular disease, the characteristics of the spinal and supraspinal components of the tremor could be used to evaluate the reduction in function or the disorder level in muscular dystrophy and Parkinson's disease, respectively.

References

Akaike H (1970) Statistical predictor identification. Ann Inst Statist Math 22:203–217

Arihara M, Sakamoto K (1999a) Contribution of motor unit activity enhanced by acute fatigue to physiological tremor of finger. Electromyogr Clin Neurophysiol 39:235–247

Arihara M, Sakamoto K (1999b) Evaluation of spectral characteristics of physiological tremor of finger based on mechanical model. Electromyogr Clin Neurophysiol 39:289–304

Bawa P, Mannard A, Stein RB (1976) Predictions and experimental tests of a visco-elastic muscle model using elastic and inertial loads. Biol Cybern 22:139–145

Cannon SC, Zahalak GI (1981) Reflex feedback in small perturbations of a limb. In: van Buskirk, WC, Woo SL-Y (eds) Proceedings of the American Society of Mechanical Engineers symposium on biomechanics, AMD, vol 43. American Society of Mechanical Engineers, New York, pp117–120

Elble RJ (1996) Central mechanisms of tremor. J Clin Neurophysiol 13:133–144

Elble RJ, Koller WC (1990) Tremor. The Johns Hopkins University Press, Baltimore

Elble RJ, Randall JE (1978) Mechanistic components of normal hand tremor. Electroencephalogr Clin Neurophysiol 44:72–82

Elble RJ, Schieber MH, Thach WT Jr (1984) Activity of muscle spindles, motor cortex and cerebellar nuclei during action tremor. Brain Res 323:330–334

Findley LJ, Koller WC (1995) Handbook of tremor disorders. Marcel Dekker, New York

Halliday AM, Redfearn JWT (1956) An analysis of the frequencies of finger tremor in healthy subjects. J Physiol (Lond) 134:600–611

Halliday DM, Conway BA, Farmer SF, Rosenberg JR (1999) Load-independent contributions from motor-unit synchronization to human physiological tremor. J Neurophysiol 82:664–675

Hasan Z (1983) A model of spindle afferent response to muscle stretch. J Neurophysiol 49:989–1006

Hömberg V, Hefter H, Reiners K, Freund H-J (1987) Differential effects of changes in mechanical limb properties on physiological and pathological tremor. J Neurol Neurosurg Psychiatry 50:568–579

Kay SM, Marple SL (1981) Spectrum analysis? – A modern perspective. Proc IEEE 69:1380–1419

Köster B, Lauk M, Timmer J, Winter T, Guschlbauer B, Glocker FX, Danek A, Deuschl G, Lücking CH (1998) Central mechanisms in human enhanced physiological tremor. Neurosci Lett 241:135–138

Kearney RE, Hunter IW (1990) System identification of human joint dynamics. Crit Rev Biomed Eng 18:55–87

Lan N, Crago PE (1994) Optimal control of antagonistic muscle stiffness during voluntary movements. Biol Cybern 71:123–135

Lenz FA, Tatton WG, Tasker RR (1983) Electromyographic response to displacement of different forelimb joints in the squirrel monkey. J Neurosci 3:783–794

Lippold OCJ (1970) Oscillation in the stretch reflex arc and the origin of the rhythmical, 8–12 c/s component of physiological tremor. J Physiol (Lond) 206:359–382

Matthews PBC, Muir RB (1980) Comparison of electromyogram spectra with force spectra during human elbow tremor. J Physiol (Lond) 302:427–441

Miao T, Sakamoto K (1995a) Effects of weight load on physiological tremor: the AR representation. Appl Human Sci 14:7–13

Miao T, Sakamoto K (1995b) Physiological tremor under pseudofraction gravity. Appl Human Sci 14:37–47

Oðuztöreli MN, Stein RB (1976) The effects of multiple reflex pathways on the oscillations in neuro-muscular systems. J Math Biol 3:87–101

Oðuztöreli MN, Stein RB (1982) Analysis of a model for antagonistic muscles. Biol Cybern 45:177–186

Oðuztöreli MN, Stein RB (1990) Optimal task performance of antagonistic muscles. Biol Cybern 64:87–94

Sakamoto K, Nishida K, Zhou L, Itakura N, Seki K, Hamba S (1992) Characteristics of physiological tremor in five fingers and evaluations of fatigue of fingers in typing. Ann Physiol Anthrop 11:61–68

Sakamoto K, Itakura N, Nishida K, Zhou L (1993) Study of function of fingers by physiological tremor. J Therm Biol 18:665–669

Sakamoto K, Miao T, Arihara M (1998) Analysis of interaction of spinal and supraspinal reflex pathways involved in physiological tremor. Electromyogr Clin Neurophysiol 38:103–113

Stein RB, Oðuztöreli MN (1976) Tremor and other oscillations in neuromuscular systems. Biol Cybern 22:147–157

Stiles RN (1976) Frequency and displacement amplitude relations for normal hand tremor. J Appl Physiol 40:44–54

Stiles RN, Randall JE (1967) Mechanical factors in human tremor frequency. J Appl Physiol 23:324–330

Watanabe A, Saito M (1984) Simulation of physiological hand tremor by two-reflex-loop theory. Biomechanism 7:32–40

Winters JM, Stark L (1987) Muscle models: what is gained and what is lost by varying model complexity. Biol Cybern 55:403–420

Zahalak GI, Cannon SC (1983) Predictions of the existence, frequency, and amplitude of physiological tremor in normal man based on measured frequency-response characteristics. J Biomech Eng 105:249–257

Zajac FE (1989) Muscle and tendon: properties, models, scaling, and application to biomechanics and motor control. Crit Rev Biomed Eng 17:359–411